IEEJ TRANSACTIONS ON ELECTRICAL AND ELECTRONIC ENGINEERING
IEEJ Trans 2018; **13**: 510–516
Published online in Wiley Online Library (wileyonlinelibrary.com). DOI:10.1002/tee.22595

Paper

A Bearing Outer Raceway Fault Detection Method in Induction Motors Based on Instantaneous Frequency of the Stator Current

Xiangjin Song[*,**], Non-member
Jingtao Hu[a*,**], Non-member
Hongyu Zhu[*,**], Non-member
Jilong Zhang[*,**], Non-member

Induction motors (IMs) are widely used in agricultural, industrial, and commercial applications. Bearing faults are one of the most common causes of breakdown in IMs. Motor current signature analysis (MCSA) is becoming a popular tool for bearing fault detection because of its cost effectiveness and noninvasiveness. However, when a motor operates under low-load and lower load conditions, MCSA cannot be used to detect the bearing outer raceway fault because of the influence of the supply frequency component spectrum leakage, eccentricity harmonics, and other noises. In this paper, a new method for the fault detection of bearing outer raceway fault in IMs is proposed. The method is based on the analysis of the instantaneous frequency (IF) of the IM stator current using Hilbert transform, and Fast Fourier Transform (FFT) spectrum analysis is used to detect the frequency associated with the bearing outer raceway fault. The proposed method can significantly reduce the negative influence of the supply frequency component spectrum leakage, and thus can enhance the fault features to detect bearing outer raceway fault under low-load and lower load conditions, compared with the traditional MCSA method. Finally, the experimental results on an IM with bearing outer raceway fault prove the effectiveness of the proposed method. © 2018 Institute of Electrical Engineers of Japan. Published by John Wiley & Sons, Inc.

Keywords: motor current signature analysis; Hilbert transform; induction motors; bearing faults; instantaneous frequency

Received 21 February 2017; Revised 25 April 2017

1. Introduction

Induction motors (IMs) play a critical role in agricultural, industrial, and commercial applications. This mainly because of their simple organizational structure, easy maintenance, premium power efficiency, and high reliability. Even though IMs are reliable, unexpected failures may still occur under environmental stresses, which could lead to production shutdown and extra maintenance cost. Thus, the online monitoring and fault diagnosis of IMs have been extensively studied to minimize financial loss [1–3].

One of the most important fault types of the IM are the bearing faults, which account for over 40% (large machines) to 90% (small machines) of all motor failures [4]. Therefore, bearing fault detection deserves serious attention.

Approaches based on vibration signal analysis have been widely used for bearing fault detection [5–7]. In recent years, bearing fault detection using motor current signature analysis (MCSA) has received considerable attention because of its low cost and noninvasive nature [1,3,8]. Several studies have been carried out for IM bearing fault detection using the IM stator current analysis. For example, Schoen *et al.* proposed a bearing fault detection model in order to derive the relationship between bearing vibration characteristics and current spectrum effects [9]. This model was then improved by Blödt *et al.* taking into consideration the radial rotor movement (amplitude modulations) and bearing-fault-related load torque variations (phase modulations) [10]. Yang *et al.* suggested independent component analysis (ICA) to detect bearing faults [1]. An algorithm for the detection of localized bearing fault, which used spectral kurtosis and envelope analysis of the stator current, was proposed by Leite *et al.* [3]. Pineda-Sanchez *et al.* applied the Teager–Kaiser energy operator (TKEO) to detect IM bearing fault under steady-state condition [11]. Wang *et al.* suggested the use of the stator current envelope via Hilbert transform to detect fault in IMs [12]. Frosini and Bassi utilized stator current analysis and IM efficiency for bearing fault detection [13]. Enzo *et al.* applied wavelet packet decomposition of the stator current to detect bearing faults [14]. Zarei and Poshtan utilized an advanced Park's vectors approach for bearing fault detection based on three-phase stator current analysis [15]. Önel *et al.* employed the Concordia transform approach for the detection of localized bearing fault in inverter-fed IMs [16]. The aforementioned technologies, however, only examine the amplitude information in bearing fault diagnosis, while spectral phase information for bearing fault detection is discarded.

In this paper, a novel method for bearing fault detection is proposed. This method is based on the analysis of the instantaneous frequency (IF) of the IM stator current using Hilbert transform, and fast Fourier transform (FFT) spectrum analysis is used to detect the frequency associated with the bearing outer raceway fault. The target frequencies are detected in the spectrum of the IF directly at their fault characteristic frequencies instead of sideband components around the supply frequency as in the traditional MCSA. Furthermore, IM speed is obtained from the spectral estimation of principal slot harmonics (PSHs). Finally, the effectiveness of the proposed method for IM bearing outer raceway fault detection is verified experimentally by IMs under different load conditions.

[a] Correspondence to: Jingtao Hu. E-mail: hujingtao@sia.cn

[*] Key Laboratory of Networked Control System, Shenyang Institute of Automation, Chinese Academy of Science, Shenyang 110016, China
[**] University of Chinese Academy of Sciences, Beijing 100039, China

The rest of the paper is organized as follows. Section 2 gives a brief description of the fault modes of a rolling-element bearing and models for fault detection using the stator current analysis. The application of Hilbert transform to extract bearing outer raceway fault characteristic frequencies from the stator current signal is presented in Section 3. Section 4 reports the experiment setup and the obtained results to verify the effectiveness of the proposed method on a three-phase IM with one artificially faulted bearing under different load conditions. Finally, some conclusions of this paper are given in Section 5.

2. Bearing Fault Modes and Fault Detection Using the Stator Current Analysis

The typical geometric structure of a rolling-element bearing is shown in Fig. 1. Such bearings are mainly composed of the outer and inner raceway, the ball elements, and the cage that ensures uniform distances between the ball elements. Under ordinary conditions, bearing faults can be separated into two types, i.e. single-point (also called localized or cyclic) and generalized-roughness (also called distributed or noncyclic) faults [17]. Generalized-roughness faults greatly worsen the entire area of a bearing element because of the absence of lubrication, erosion, or bearing pollution and are hard to represent by specific frequencies [17,18]. Unlike generalized-roughness faults, localized faults affect a localized region, which usually can be imagined as a small hole, a pit, or a missing piece of material on the bearing surface, and they can be characterized by specific fault-related frequencies [10,17]. When a localized faulted bearing runs at a constant speed, a periodic impact between the rolling elements and the raceway is produced [19,20]. The existence of such impulsive forces gives rise to an increase in the vibrational level [13,19]. The frequencies of these vibrations are predictable and rely on the fault location, bearing geometry, and operating speed [13,15]. In this paper, only localized faults are studied.

Localized faults can be usually divided into four categories depending on the affected element, namely outer raceway fault, inner raceway fault, ball fault, and cage fault. When the outer raceway is stationary, the vibrational characteristic frequencies of these faults can be expressed as [21]

$$f_{of} = \frac{N_b}{2} f_r \left(1 - \frac{D_b}{D_c} \cos\beta\right) \tag{1}$$

$$f_{if} = \frac{N_b}{2} f_r \left(1 + \frac{D_b}{D_c} \cos\beta\right) \tag{2}$$

$$f_{bf} = \frac{D_c}{D_b} f_r \left(1 - \left(\frac{D_b}{D_c} \cos\beta\right)^2\right) \tag{3}$$

$$f_{cf} = \frac{1}{2} f_r \left(1 - \frac{D_b}{D_c} \cos\beta\right) \tag{4}$$

where f_{of} is the outer raceway fault frequency, f_{if} is the inner raceway fault frequency, f_{bf} is the ball fault frequency, f_{cf} is the cage fault frequency, f_r is the rotor rotational frequency, N_b is the number of balls, D_b is the ball diameter, D_c is the ball pitch diameter, and β is the contact angle between a ball and the raceway.

For the bearings with 6–12 rolling elements, the outer and inner raceway fault frequencies can be approximately computed as [22]

$$f_{of} = 0.4 N_b f_r \tag{5}$$

$$f_{if} = 0.6 N_b f_r \tag{6}$$

Since the rotor is supported by the rolling-element bearings, any vibrations due to bearing faults will cause a radial motion between the rotor and the stator, which then changes the air gap flux density and machine inductance like eccentricity faults; finally, these anomalies result in the modulation of the stator current [1,15]. The relationship between bearing vibration frequencies and current frequencies was first proposed by Schoen *et al.* based on the generation of rotating eccentricities at bearing fault characteristic frequencies. For example, for an outer raceway fault, the vibration characteristic frequency f_{of} is reflected in the current spectrum as [9]

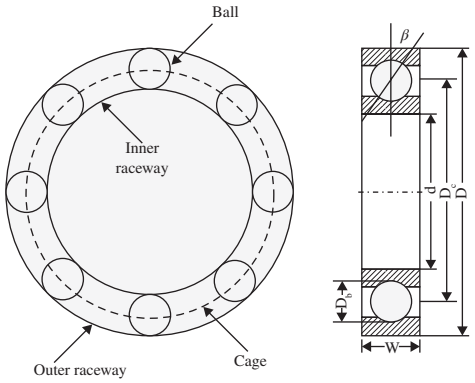

Fig. 1. Typical structure of a rolling-element bearing with main parameters

$$f_{co} = f_1 \pm n f_{of} \tag{7}$$

where f_{co} is the bearing fault current harmonic frequencies, f_1 is the fundamental supply frequency, and $n = 1, 2, 3\ldots$ is the harmonic indexes. Another new mathematical model for bearing fault detection was proposed by Blödt *et al.* taking into consideration not only the radial motion between rotor and stator but also the bearing-fault-related load-torque variations [10]. Blödt considered the fault-related torque variations as phase modulations. These phase modulations can also be used for bearing fault detection.

In a rolling-element bearing, the stationary ring (outer raceway in this case) fault happens first due to the fact that the stationary ring material in the load area receives more dynamic load cycles than other bearing components (e.g. the rotating ring and rolling elements) [2]. Hence, the outer raceway fault detection is within the scope of investigations.

From (5), we can see that the speed of the IM is needed in order to determine the bearing outer raceway fault characteristic frequency. In this paper, the IM speed $f_r = (f_{sh} - f_1)/R$ (R is the number of rotor slots in IM) is obtained from the spectral estimation of PSH, f_{sh}.

3. Proposed Bearing Outer Raceway Fault Detection Scheme Based on Instantaneous Frequency

As mentioned, the spectral amplitude information of the stator current has been fully applied in previous works for bearing fault detection, whereas techniques relying on phase information have been ignored. In this section, a new bearing outer raceway fault detection method taking advantage of phase information is introduced. First, the principal concept of IF is introduced, and then its application to the stator current analysis of a faulty motor is discussed. Finally, the bearing outer raceway fault detection scheme is proposed.

3.1. Instantaneous frequency The notion of IF is mostly used in communications, and a review of the theoretical treatment of IF can be found in Boashash [23,24]. The IF of a real

continuous-time signal $x(t)$ is defined as the time derivative of the instantaneous phase of the analytic signal obtained from Hilbert transform [24–26].

In order to obtain the instantaneous phase of the real signal $x(t)$, we need to perform the Hilbert transform of the signal $x(t)$ first. The Hilbert transform $\widehat{x}(t)$ of a real signal $x(t)$ is given by [26,27]

$$\widehat{x}(t) = H(x(t)) = \frac{1}{\pi}\int_{-\infty}^{\infty}\frac{x(\tau)}{t-\tau}\mathrm{d}\tau = x(t) * \frac{1}{\pi t} \tag{8}$$

where $H(\cdot)$ means the Hilbert operator, and * represents the convolution operator. By combining the $x(t)$ and $\widehat{x}(t)$, the analytic signal of the real signal $x(t)$ is obtained as

$$z(t) = x(t) + j\widehat{x}(t) = a(t)e^{j\varphi(t)} \tag{9}$$

where $a(t) = \sqrt{x^2(t) + \widehat{x}^2(t)}$ is the instantaneous envelope of $z(t)$, which contains important information of the energy of $x(t)$, and $\varphi(t) = \arctan(\widehat{x}(t)/x(t))$ is the instantaneous phase of $z(t)$.

From the instantaneous phase $\phi(t)$ of the analytic signal, we can get the IF $f_{if}(t)$ of the real signal $x(t)$ as

$$f_{if}(t) = \frac{1}{2\pi}\frac{\mathrm{d}\varphi(t)}{\mathrm{d}t} \tag{10}$$

The technique for extracting the IF of a faulty motor current is introduced in the next section.

3.2. Instantaneous frequency of the stator current in a faulty motor The single-phase stator current in an ideal motor can be expressed by

$$i_h(t) = I_1\cos(w_1 t) = I_1\cos(2\pi f_1 t) \tag{11}$$

where I_1 is the fundamental value of the stator current, and $w_1 = 2\pi f_1$ is the supply angular frequency.

If an IM with bearing outer raceway fault runs at a constant speed, a single-phase stator current, which only contains phase modulation, can be written as

$$i_{mp}(t) = I_1\cos(w_1 t + p(t)) \tag{12}$$

where $p(t) = m\cos(w_{of}t)$, and $w_{of} = 2\pi f_{of}$. Here, $p(t)$ means the phase modulation caused by the fault-related torque variations, and m denotes the modulation depth.

Then the Hilbert transform of (12) is constructed by changing the cosine function to sine function:

$$H(i_{mp}(t)) = I_1\sin(w_1 t + m\cos(w_{of}t)) \tag{13}$$

By combing (12) and (13), we can get the analytical signal relevant to $i_{mp}(t)$:

$$z_{mp}(t) = i_{mp}(t) + jH(i_{mp}(t)) = I_1 e^{j(w_1 t + m\cos(w_{of}t))} \tag{14}$$

From the analytical signal of $z_{mp}(t)$, we can get the instantaneous phase $\phi_{mp}(t)$ of the stator current in a faulty motor as

$$\varphi_{mp}(t) = w_1 t + m\cos(w_{of}t) \tag{15}$$

The IF of the stator current in a faulty motor can be calculated as the derivative of the instantaneous phase:

$$f_{ifmp}(t) = \frac{1}{2\pi}\frac{d\varphi_{mp}(t)}{dt} = f_1 - mf_{of}\sin(w_{of}t) \tag{16}$$

By comparing of (15) and (16), we can see that the bearing fault characteristic frequency w_{of} is disturbed by the fundamental supply frequency $w_1 t$ in (15), so the instantaneous phase cannot be directly used for bearing outer raceway fault detection. However, the effect of the fundamental supply frequency is eliminated in (16). Moreover, the demodulation procedure has transferred the sideband component characteristic frequency $|f_1 \pm f_{of}|$ to the fault characteristic frequency f_{of}. Therefore, the bearing outer raceway fault characteristic frequency f_{of} can be clearly identified in the spectrum of IF of the sampled stator current in a faulty IM. In this paper, the proposed method for bearing outer raceway fault detection relies on the analysis of IF.

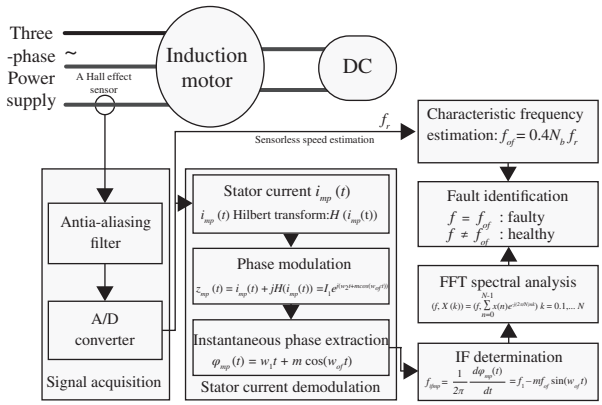

Fig. 2. Schematic diagram of the proposed bearing outer raceway fault detection method

3.3. Schematic diagram of the proposed bearing outer raceway fault detection method The bearing outer raceway fault detection diagram proposed in this paper is shown in Fig. 2. This fault detection method has the following six components: signal acquisition, stator current demodulation, IF determination, characteristic frequency estimation, FFT spectral analysis, and fault identification. The stator current in one of the three phases in the IM is colleected by the signal acquisition component and sent to the stator current demodulation component, where the obtained current signal is demodulated using Hilbert transform and the instantaneous phase is extracted. In the IF determination component, the IF can be calculated as the derivative of the instantaneous phase. The speed of the IM is estimated by PSH detection, and then the bearing outer raceway characteristic frequency can be obtained. Depending on whether the characteristic frequency can be found in the FFT spectrum of IF, the conclusion of failure or not can be drawn.

4. Experimental Verification

This section is divided into two parts: first, an overview of the experimental test rig is presented, and an artificially produced bearing localized fault is introduced by drilling a hole in the bearing outer raceway, which is similar to other well-known studies [3,13,14]. Then the proposed bearing outer raceway fault detection method is verified using the sampled stator current signals.

4.1. Test rig A schematic diagram of the experimental test rig used in this paper is shown in Fig. 3.

The rated data of the tested IM are given in Table I. The IM is mechanically coupled to a DC machine, which feeds an external resistor bank. The motor can be identically loaded at different speeds from zero to the rated load by adjusting the field voltage of the DC machine. Both machines are fixed on a steel plate test bench resting on a cement floor. The National Instrument data acquisition (NI DAQ 6216) card used in this test accepts only voltage signal with maximum amplitudes of ±10 V. A JLB-21 Hall-effect current sensor is used to collect the current signal first, and then the acquired current signal is converted to proportional voltage signals by the conditioning circuit. A PC equipped with

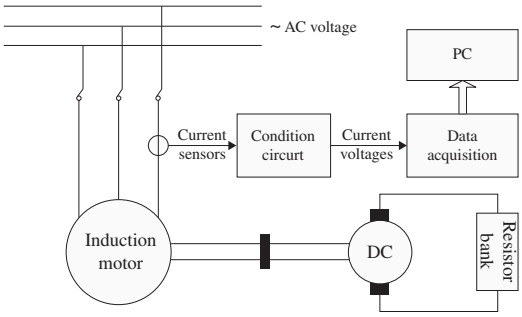

Fig. 3. Schematic of the experimental test rig

Table I. Test induction motor rated parameters

Nominal power	3 kW
Nominal rated voltage	380 V
Nominal rated current	6.8A
Frequency	50 Hz
Pole pairs	2
Stator slots	36
Rotor slots	32
Stator winding connection	Y

Fig. 4. Photograph of the experimental setup used for bearing fault detection

a DAQ card through a USB cable is used to store the signals in the memory. A picture of the experimental setup is shown in Fig. 4.

The induction machine has two CU6206RZ-type bearings (single-row, deep groove ball bearings) with width $w = 16$ mm, outside diameter $D = 62$ mm, inside diameter $d = 30$ mm, and pitch diameter $D_c = 46.0$ mm. Each bearing has nine balls ($N_b = 9$) with a diameter of $D_b = 9.52$ mm. The contact angle of the ball with the race (β) is assumed to 0°. Two identical motors are prepared: one motor carries healthy bearings and the other one carries a faulty bearing, which are mounted on the load side of the mechanics. Here, a 6-mm-diameter hole is drilled through the outer race of the bearing to simulate a localized fault. Figure 5 shows the healthy and faulted bearings used in the experimental setup.

In the experiments, tests were performed with the faulty motor under five different loads (higher, high, medium, low and lower) by randomly adjusting the field voltage of the DC machine. For the sake of spectral contrast analysis, a supplementary test was performed with the healthy motor in high load condition. In each case, 25 s of a phase stator current is sampled at 25 kHz. Table II summarizes the load conditions of the six experimental tests including the estimated speeds by means of PSH detection,

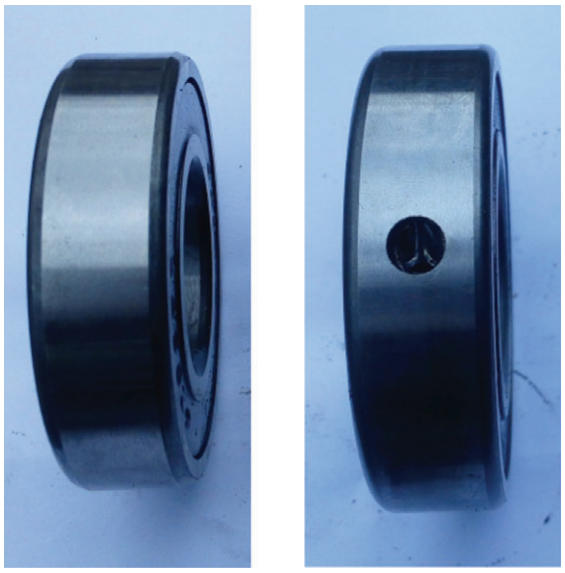

(a) (b)

Fig. 5. Tested bearings: (a) Healthy (b) outer raceway fault

and theoretical values of the sideband components associated with the outer raceway fault.

In Table II, f_1 denotes the estimated fundamental supply frequency, f_{sh} denotes the estimated PSH frequency, f_r denotes the estimated speed, $f_{of} = 3.6 f_r$ denotes the theoretical bearing outer raceway characteristic frequency, and $|f_1 \pm f_{of}|$ denotes the theoretical fault sideband components.

4.2. Experimental results To assess the effectiveness of the proposed method for IM bearing outer raceway fault detection, two types of spectra are presented for comparison in this paper: (i) FFT of the stator current (the traditional MCSA method), and (ii) FFT of $f_{ifmp}(t)$, the IF of the stator current's analytic signal (the proposed method).

Initially, the experimental stator current spectra (0–150 Hz) corresponding to the healthy IM and the IM with the bearing outer raceway fault are analyzed. We can see the frequency components at $f_1 \pm f_r$ from Fig. 6(a). These components are present in healthy IM because of the inherent level of eccentricity. Comparisons of Fig. 6(a) and (b) show that there has been an increase in the number and the magnitude of eccentricity harmonics in Fig. 6(b), which are caused by the fault in the bearing outer raceway. Because of the spectral leakage of the supply frequency f_1 and the influence of eccentricity harmonics and other noises, the characteristic sideband frequency $|f_1 - f_{of}|$ is completely buried and only $f_1 + f_{of}$ is visible. However, the frequency $f_1 + f_{of}$ is also difficult to recognize because of the spectral leakage of the supply frequency and the influence of eccentricity harmonics and other noises as the level of load decreases. Demodulation of the stator current is used to improve the spectral leakage and also to monitor the characteristic frequency f_{of} instead of the sideband component around the supply frequency $f_1 + f_{of}$. In order to improve clarity of the figures (see below), linear plots instead of logarithmic plots have been adopted.

The time-domain signals of instantaneous phase and IF of the stator current in a faulty IM under high-load condition and their FFT spectrum are illustrated in Figs 7 and 8, respectively. From Fig. 7(a), we can see that the amplitude of the instantaneous phase signal grows with time because of the influence of the item $w_1 t$. Comparisons of Fig. 8(a) and (b) indicate that the characteristic frequency f_{of} is not present in the FFT spectrum of instantaneous phase but is included in the FFT spectrum of

Table II. Theoretical fault sideband components of the healthy and faulty motor

Motor condition	Load	f_1 (Hz)	f_{sh} (Hz)	f_r (Hz)	$f_{of} = 3.6 f_r$ (Hz)	$\lvert f_1 \pm f_{of} \rvert$ (Hz)
Healthy	(a) High	50.07	821.30	24.10	—	—
	(b) Lower	50.02	841.50	24.73	89.03	39.01,139.05
	(c) Low	50.07	839.00	24.65	88.74	38.67,138.81
Faulty (outer raceway fault)	(d) Medium	50.02	828.00	24.31	87.52	37.50,137.54
	(e) High	50.07	821.10	24.09	86.72	36.65,136.79
	(f) Higher	50.07	813.70	23.86	85.90	35.83,135.97

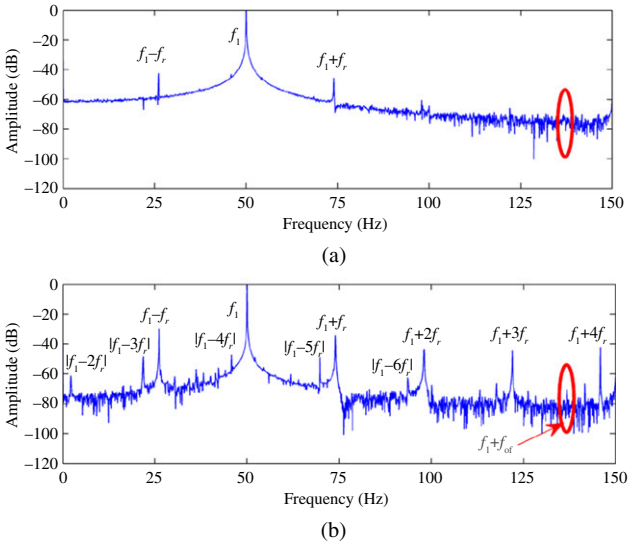

Fig. 6. FFT spectra of the stator current (0–150 Hz) under high-load condition: (a) Healthy IM (b) IM with bearing outer raceway fault

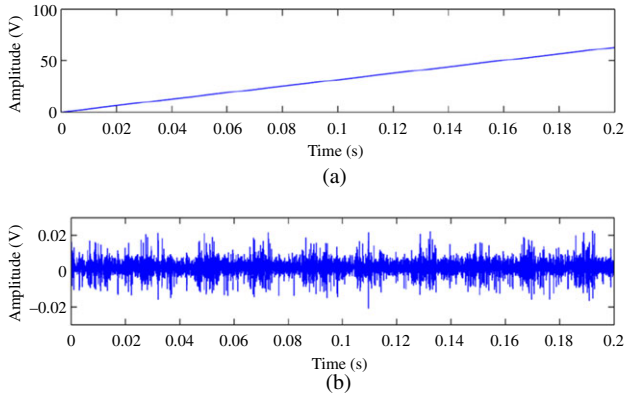

Fig. 7. Time-domain signals (0–0.2 s) under high-load condition: (a) Instantaneous phase (b) IF of the stator current in a faulty induction motor

IF. These results are consistent with the theoretical derivation. Therefore, the IF of the stator current can be used for bearing fault detection. In this paper, the IF of the stator current is used to detect bearing outer raceway fault and the spectral results of the stator current and IF for bearing outer raceway fault detection are compared.

From Fig. 7(b), we can see that the IF signals is no longer a pure sine function. Therefore, other harmonics that have no connection with the bearing outer raceway fault are able to show up in the spectrum (Fig. 8(b)). Their appearance may be due to mechanical resonances, supply harmonics, etc. However, they do not disturb the bearing fault detection because of the diagnosis is carried out

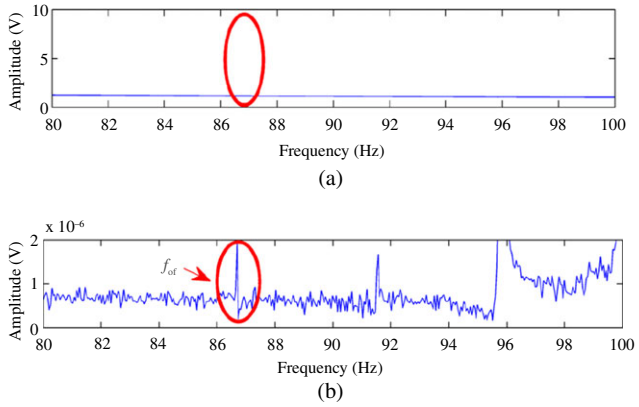

Fig. 8. Frequency-domain signals (0–0.2 s) under high-load condition: (a) Instantaneous phase (b) IF of the stator current in a faulty induction motor

by using the peak detection at the fault characteristic frequency f_{of}, which can be computed by (5) after the IM speed is obtained.

Figure 9 presents the FFT spectra of the stator current near the characteristic sideband frequency $f_1 + f_{of}$ for the case of the healthy motor under high-load condition and for the case of the motor with bearing outer raceway fault under the five different load conditions. As the level of load decreases, so does the amplitude of the characteristic sideband frequency. In the case of the lower load and low-load tests, the fault characteristic sideband frequency $f_1 + f_{of}$ is completely buried under the spectral leakage of the supply frequency, eccentricity harmonics, and other noises. In these cases, the FFT spectrum of the stator current is unable to correctly diagnose the bearing outer raceway fault.

In order to verify the effectiveness of the proposed method, the same tested stator current of the IM that was analyzed using the traditional MCSA was processed by the Hilbert transform before performing FFT. Figure 10 shows the FFT spectrums of the proposed signal $f_{ifmp}(t)$ near the characteristic frequency f_{of} for the case of the healthy motor under high-load condition and for the case of the motor with bearing outer raceway fault under the five different load conditions. Comparing the results of Figs 9 and 10, the desired frequency is detected in the spectra of the proposed signal $f_{ifmp}(t)$ precisely at its characteristic frequency f_{of} instead of sideband component around the supply frequency $f_1 + f_{of}$ as in the traditional MCSA. The leakage from the supply frequency has been reduced from these spectra. Thus, the proposed method can be used to detect the characteristic frequency f_{of} directly associated with the bearing outer raceway fault under these different load conditions.

5. Conclusion

A new method was proposed for bearing outer raceway fault detection using IF of stator current signal based on the Hilbert transform with FFT spectrum analysis. The Hilbert transform was introduced to obtain the IF of the phase current, which contained

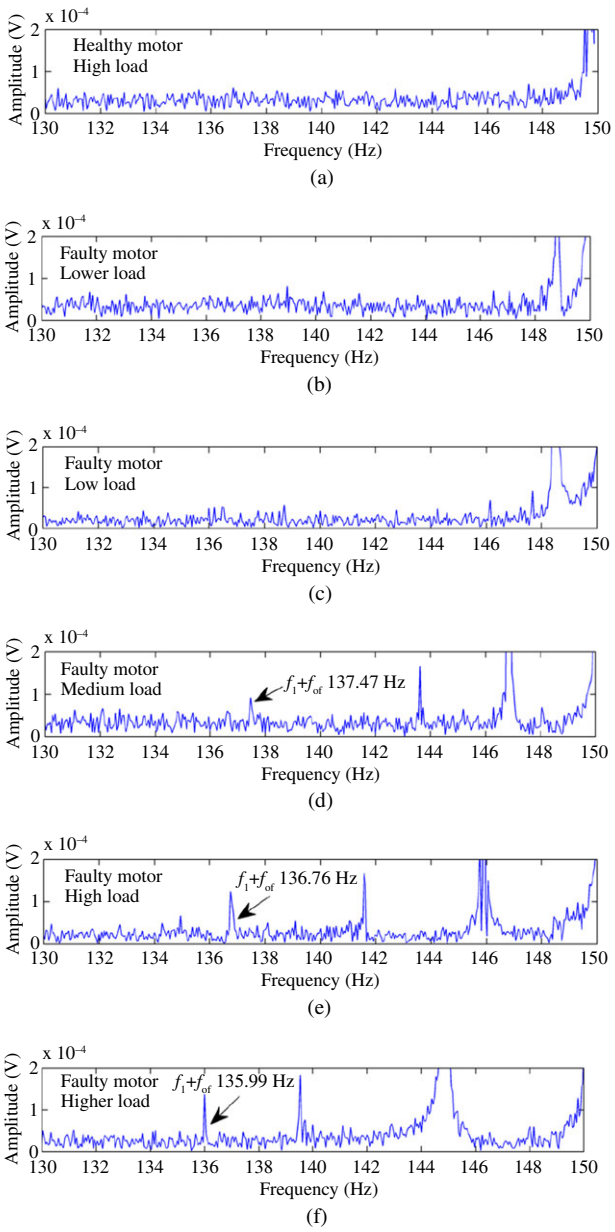

Fig. 9. FFT spectra of the stator current under six different tests: high loaded healthy motor, and motor with outer raceway fault under five different load conditions: (a) High loaded healthy motor (b) lower load (c) low load (d) medium load (e) high load (f) higher load

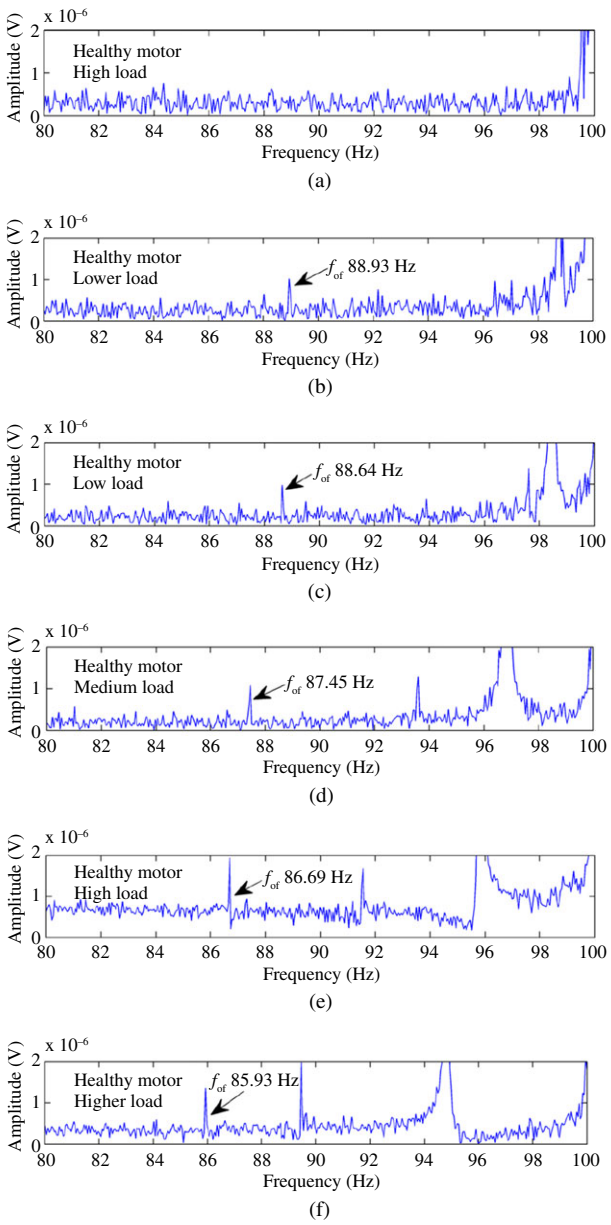

Fig. 10. FFT spectra of the instantaneous frequency under six different tests: high loaded healthy motor, and motor with outer raceway fault under five different load conditions: (a) High loaded healthy motor (b) lower load (c) low load (d) medium load (e) high load (f) higher load

the bearing outer raceway characteristic frequency. The FFT spectrum analysis was then performed to detect the characteristic frequency. The proposed method could significantly reduce the negative influence of supply frequency component spectral leakage and thus enhance the fault features to detect bearing outer raceway fault under low-load and lower load conditions, compared with the traditional MCSA method. Finally, the effectiveness of the proposed method was verified by using IM bearing outer raceway fault detection. Experimental results showed that the IF is effective for bearing outer raceway fault detection under different load conditions.

Additional investigations are under way to find a suitable combination method of Hilbert transform and high-resolution techniques to detect bearing outer raceway fault, which will be helpful to reduce computational expense. Furthermore, different degrees of bearing faults should also be included in our study, so that we can evaluate the severity of the bearing faults. Therefore, this method will be feasible and effective to achieve the online monitoring and diagnosis of bearing outer raceway fault.

Acknowledgments

This work was supported by the National Key Research and Development Program of China (grant number 2016YFD0700105) and the Key Research Program of the Chinese Academy of Sciences (grant number KFZD-SW-415).

References

(1) Yang T, Pen H, Wang Z, Chang C-S. Feature knowledge based fault detection of induction motors through the analysis of stator current data. *IEEE Transactions on Instrumentation & Measurement* 2016; **65**(3):549–558.

(2) Li DZ, Wang W, Ismail F. A spectrum synch technique for induction motor health condition monitoring. *IEEE Transactions on Energy Conversion* 2015; **30**(4):1348–1355.
(3) Leite VCMN, Borges dSJG, Veloso GFC, Borges dSLE. Detection of localized bearing faults in induction machines by spectral kurtosis and envelope analysis of stator current. *IEEE Transactions on Industrial Electronics* 2015; **62**(3):1855–1865.
(4) Riera-Guasp M, Antonino-Daviu J, Capolino GA. Advances in electrical machine, power electronic, and drive condition monitoring and fault detection: State of the art. *IEEE Transactions on Industrial Electronics* 2015; **62**(3):1746–1759.
(5) Maruthi G, Hegde V. Application of MEMS accelerometer for detection and diagnosis of multiple faults in the roller element bearings of three phase induction motor. *IEEE Sensors Journal* 2016; **16**(1):145–152.
(6) Harmouche J, Delpha C, Diallo D. Improved fault diagnosis of ball bearings based on the global spectrum of vibration signal. *IEEE Transactions on Energy Conversion* 2015; **30**(1):376–383.
(7) Zarei J, Tajeddini MA, Karimi HR. Vibration analysis for bearing fault detection and classification using an intelligent filter. *Mechatronics* 2014; **24**(2):151–157.
(8) Bouchikhi EHE, Choqueuse V, Benbouzid M. Induction machine faults detection using stator current parametric spectral estimation. *Mechanical Systems and Signal Processing* 2015; **52-53**:447–464.
(9) Schoen RR, Habetler TG, Kamran F, Bartfield RG. Motor bearing damage detection using stator current monitoring. *IEEE Transactions on Industry Applications* 1995; **31**(6):1274–1279.
(10) Blödt M, Granjon P, Raison B, Rostaing G. Models for bearing damage detection in induction motors using stator current monitoring. *IEEE Transactions on Industrial Electronics* 2008; **55**(4):1813–1822.
(11) Pineda-Sanchez M, Puche-Panadero R, Riera-Guasp M, Perez-Cruz J, Roger-Folch J, Pons-Llinares J, Climente-Alarcon V, Antonino-Daviu JA. Application of the Teager-Kaiser energy operator to the fault diagnosis of induction motors. *IEEE Transactions on Energy Conversion* 2013; **28**(4):1036–1044.
(12) Wang J, Liu S, Gao R-X, Yan R. Current envelope analysis for defect identification and diagnosis in induction motors. *Journal of Manufacturing Systems* 2012; **31**(4):380–387.
(13) Frosini L, Bassi E. Stator current and motor efficiency as indicators for different types of bearing faults in induction motors. *IEEE Transactions on Industrial Electronics* 2010; **57**(1): 244–251.
(14) Lau ECC, Ngan HW. Detection of motor bearing outer raceway defect by wavelet packet transformed motor current signature analysis. *IEEE Transactions on Instrumentation and Measurement* 2010; **59**(10):2683–2690.
(15) Zarei J, Poshtan J. An advanced Park's vectors approach for bearing fault detection. *Tribology International* 2009; **42**(2):213–219.
(16) Önel İY, Ayçiçek E, Şenol İ. An experimental study, about detection of bearing defects in inverter fed small induction motors by Concordia transform. *Journal of Intelligent Manufacturing* 2009; **20**(2):243–247.
(17) Stack JR, Habetler TG, Harley RG. Fault classification and fault signature production for rolling element bearings in electric machines. *IEEE Transactions on Industry Applications* 2004; **40**(3): 735–739.
(18) Immovilli F, Cocconcelli M, Bellini A, Rubini R. Detection of generalized-roughness bearing fault by spectral-kurtosis energy of vibration or current signals. *IEEE Transactions on Industrial Electronics* 2009; **56**(11):4710–4717.
(19) Bediaga I, Mendizabal X, Arnaiz A, Munoa J. Ball bearing damage detection using traditional signal processing algorithms. *IEEE Instrumentation & Measurement Magazine* 2013; **16**(2):20–25.
(20) Immovilli F, Bellini A, Rubini R, Tassoni C. Diagnosis of bearing faults in induction machines by vibration or current signals: A critical comparison. *IEEE Transactions on Industry Applications* 2010; **46**(4):1350–1359.
(21) Li B, Chow MY, Tipsuwan Y, Hung JC. Neural-network-based motor rolling bearing fault diagnosis. *IEEE Transactions on Industrial Electronics* 2000; **47**(5):1060–1069.
(22) Schiltz RL. Forcing frequency identification of rolling element bearings. *Sound and vibration* 1990; **24**(5):16–19.
(23) Boashash B. Estimating and interpreting the instantaneous frequency of a signal. I. Fundamentals. *Proceedings of the IEEE* 1992; **80**(4):520–538.
(24) Boashash B. Estimating and interpreting the instantaneous frequency of a signal. II. Algorithms and applications. *Proceedings of the IEEE* 1992; **80**(4):540–568.
(25) Soualhi A, Medjaher K, Zerhouni N. Bearing health monitoring based on hilbert–huang transform, support vector machine, and regression. *IEEE Transactions on Instrumentation and Measurement* 2015; **64**(1):52–62.
(26) Cheng G, Cheng Y-L, Shen L-H, Qiu J-B, Zhang S. Gear fault identification based on Hilbert–Huang transform and SOM neural network. *Measurement* 2013; **46**(3):1137–1146.
(27) Georgoulas G, Loutas T, Stylios CD, Kostopoulos V. Bearing fault detection based on hybrid ensemble detector and empirical mode decomposition. *Mechanical Systems and Signal Processing* 2013; **41**(1):510–525.

Xiangjin Song (Non-member) received the B.Sc. degree in automation from Zhengzhou University, Zhengzhou, China, in 2012. She is currently pursuing the Ph.D. degree in measurement technique and automation equipment at Shenyang Institute of Automation (SIA), Chinese Academy of Sciences and she is a Ph.D. student in the University of Chinese Academy of Sciences. Her research interests include condition monitoring and fault diagnosis of electrical machines.

Jingtao Hu (Non-member) received the B.Sc. and M.Sc. degrees from Dalian University of Technology, Dalian, China, in 1985 and 1988, respectively. He is currently a Research Fellow with Shenyang Institute of Automation (SIA), Chinese Academy of Sciences, and a Professor and Doctoral Supervisor in the University of Chinese Academy of Sciences. His research interests include the remote equipment condition monitoring and fault diagnosis.

Hongyu Zhu (Non-member) received the M.Sc. degree from Shenyang University of Technology, Shenyang, China, in 2006, and the Ph.D. degree in mechanical and electronic engineering from Shenyang Institute of Automation, Chinese Academy of Sciences, Shenyang, in 2014. He is currently an Associate Professor with the University of Science and Technology, Liaoning. His research interests include condition monitoring and fault diagnosis of electrical machines.

Jilong Zhang (Non-member) received the B.S. degree in mechanical engineering from Dalian Railway Institute, Dalian, China, in 2002, and the M.S. degree in mechatronic engineering from Dalian University of Technology, Dalian, in 2006. He is currently an Associate Professor with Shenyang Institute of Automation (SIA), Chinese Academy of Sciences. His current research interests include manufacturing system modeling and control, industrial safety, and fault diagnosis of electrical machines.